Environmental Science and Pollution Research (2023) 30:3942–3952
https://doi.org/10.1007/s11356-022-22404-2

RESEARCH ARTICLE

A novel design for solar collector used for water heating application having nanofluid as working medium: CFD modeling and simulation

Rajneesh Kumar[1] · Manjeet Kharub[2] · Rajesh Sharma[1] · Periapattana Nagaraj Hrisheekesha[1] · Varun Goel[3] · Suvanjan Bhattacharyya[4] · Vineet Veer Tyagi[5] · Varun[6]

Received: 4 March 2022 / Accepted: 1 August 2022 / Published online: 12 August 2022

Abstract

A solar collector is a simple and cheap device that converts solar radiation into valuable heat energy. The thermal performance of the solar collectors can be enhanced significantly with the suspension of nanoparticles in the base fluid. A novel design for a solar-assisted water heater (SWH) is proposed in the current study, and the effect of nanofluid has been investigated on the thermal efficiency of the SWH. The use of nanofluid is one of the prominent methods in comparison to other techniques for improving the performance of solar collectors. Therefore, the base working fluid, i.e., water is mixed with the alumina nanoparticles of average particle size of 30 nm, and they are assumed to be spherical. The flow and thermal characteristics of nanofluid through the solar water heater are simulated numerically with the help of the Eulerian–Eulerian two-phase model using the finite volume method (FVM). The commercial package ANSYS Fluent, is used for modeling the problem under transient conditions with a pressure-based solver. In comparison to a conventional flat plate collector, the proposed solar water heater consists of a corrugated absorber-plate and the effect of the radius of curvature has been investigated on the heat transfer and collector efficiency. With the proposed design, the heat transfer area available with the riser tubes increases remarkably and it leads to a 43% and 14% increase in heat transfer augmentation and collector efficiency, in comparison to the conventional solar water heater.

Keywords Solar collector · Nanofluid · Solar water heater · Collector efficiency · Corrugated plate solar collector

Nomenclature

A	Area (m^2)
C_p	Specific heat (J kg^{-1} K^{-1})
D	Diameter (riser tube) (m)
h_v	Coefficient of volumetric heat transfer (W $(m^2$ $K)^{-1}$)
I	Solar intensity (W m^{-2})
K_B	Stefan–Boltzmann coefficient (W m^{-2} K^{-4})
L	Length (m)
m	Mass flow rate (kg s^{-1})
Nu	Nusselt number (dimensionless)
Pr	Prandtl number
Q	Energy (W)
Re	Reynolds number (dimensionless)
T	Temperature (K)
v	Velocity
W	Width (m)

Subscripts

a	Average
c	Collector
f	Base fluid
i	Inlet
l	Loss
n	Nanoparticles
o	Outlet
s	Surrounding
u	Useful

Responsible Editor: Philippe Garrigues

✉ Manjeet Kharub
manjeetkharub@gmail.com

[1] Mechanical Engineering Department, Chandigarh Engineering College Landran, Punjab, India

[2] Mechanical Engineering Department, CVR College of Engineering, Hyderabad, India

[3] Mechanical Engineering Department, National Institute of Technology Hamirpur, Hamirpur 177001, India

[4] Department of Mechanical Engineering, BITS Pilani, Pilani, India

[5] School of Energy Management, Shri Mata Vaishno Devi University, Katra, Jammu, India

[6] Govt. Polytechnic Kangra (HP), Kangra, India

Greek symbols

μ Viscosity (kg m^{-1} s^{-1})
ρ Density (kg m^{-3})
φ Volume fraction (dimensionless)

Introduction

In the past few centuries, the energy demand has mostly been fulfilled using fossil fuels only. According to the World Energy Outlook report, more than 70% of global power production is done by fossil fuels, and among it, 38% of power is harvested by coal only (World Energy Outlook 2019). These fuels are non-renewable sources of energy and will be going to last in the next 50 years (Kalogirou 2009). More importantly, the carbon dioxide and carbon monoxide released due to the combustion of these fuels results in global warming, climate change, etc., which are directly responsible for causing the melting of glaciers (or rising sea water level), floods, droughts, etc. This reason motivated the research community to find alternate energy sources which are eco-friendly, clean, and non-exhaustible. Renewable energy sources like solar energy, wind energy, geothermal energy, etc. are the best alternatives for fossil fuels as these are freely available and environment friendly. As per the International Renewable Energy Agency (IRENA), it is projected to increase global power production using renewable energy by up to 40% by 2049 (IRENA 2018). Thus, there is a lot of scope in the renewable energy sector and there is a need for time to design and develop improved systems for harvesting renewable energy.

Solar energy is present abundantly and almost everywhere on Earth, and there is no carbon generation taking place while harvesting energy from solar energy. The heat exchanger used for harvesting thermal energy from solar radiation is called a solar collector, and it is simple in design, low cost of manufacturing, durable, and reliable. For the low-temperature range, the flat-plate solar collector is used (Kalogirou 2009). The working fluid can be either air or water depending on the purpose of use. With the use of solar water heaters, the water heating cost can be reduced by 70% in domestic applications, and more importantly, it is almost maintenance-free (Jobair et al. 2018). Usually, the thermal performance of the solar collectors is not up to the mark because of the constructional, material, and working constraints (Kumar et al. 2020; Goel et al. 2021). Different techniques can be used for improving the performance of solar collectors like artificial roughnesses (Azari et al. 2021), fins, and baffles (Abo-Elfadl et al. 2021), jet impingement (Goel and Singh 2021), nanofluids (GaneshKumar et al. 2022), etc. Among all other techniques, the properties of the working fluid can be improved considerably with the suspension of the nano-sized particles in the base fluid (Choi 1995). In the case of nanofluids, the nanoparticles have relatively higher heat-conducting properties, and when these particles are suspended in the base fluid, it collectively enhances the thermophysical properties of the working fluid (Xuan and Li 2020).

Many studies (both experimental and theoretical) have been performed by different researchers using different types of nanofluids (Eastman et al. 2001; Ali et al. 2003; Shafahi et al. 2010; Zhu et al. 2011; Sasikumar et al. 2020). There are different parameters like the conductivity of base fluid and nanoparticles, and the volume fraction of nanoparticles plays a vital role in deciding the thermal conductivity of nanofluid (Natarajan and Sathish 2009). With the 0.05% concentration of CuO nanoparticles, the thermal performance of the solar collector can be improved by 6.3% (Michael and Iniyan 2015). In another study, the 25-nm-sized Cu nanoparticles with 0.1% weight concentration in water resulted in a 23.83% increase in the solar collector efficiency (He et al. 2015). The effect of metal (Cu) and metal oxide (CuO) on the thermal conductivity of nanofluid has been investigated by Milanese et al. (2016). The two layers of the water molecules formed around the Cu nanoparticles (called the layering phenomenon) which resulted in higher thermal conductivity of the Cu-based nanofluid in comparison to CuO-based nanofluid. Iacobazzi et al. (2016) have analyzed the effect of Brownian motion, thermal boundary resistance, clustering, etc. on the thermal conductivity of the Al_2O_3-based nanofluid. Among all other mechanisms, the mass difference scattering is the most intensive which reduces the thermal conductivity of the nanofluid. Sundar et al. (2020) have considered the wire coil rod insert in a solar collector having an Al_2O_3–water nanofluid. The different concentrations of Al_2O_3 nanoparticles are used which varied from 0.1 to 0.3%. The maximum efficiency of the collector obtained is 37.73% at nanoparticles concentration of 0.3%, and while a wire coil rod is inserted in the system, the collector efficiency further improved to 64.15%. The thermal conductivity of the Al_2O_3–water nanofluid not only increased with the volume fraction but also improved with the temperature, and it is reported that at a volume fraction of 1%, the thermal conductivity improved by 2% at 21 °C and 10.8% at 10.8 °C (Das et al. 2006). In an experimental study, Pang et al. (2012) reported that the thermal conductivity of Al_2O_3–methanol nanofluid was found maximum which is 10.7% (at 20 °C and 0.5% volume fraction) higher than the base medium. Eidan et al. (2018) have used acetone as base fluid, and nanoparticles of Al_2O_3 and CuO are suspended in it with the volumetric concentration of 0.25 and 0.5%, respectively. Under experimental conditions, it is noticed that with the use of higher volumetric concentration, the CuO nanoparticles get settled down more frequently in comparison to the

Al_2O_3. The efficiency of the solar collector was claimed to be higher with the use of nanofluids than the acetone only, and it increases with the increase of volume concentration from 0.25 to 0.5%. Huang and Marefati (2020) have investigated the influence of Al_2O_3 and CuO nanoparticles on the efficiency of different types of solar collectors (that are the flat-plate and parabolic trough, parabolic dish collector, and linear Fresnel solar reflector) in two different base fluids, i.e., water and Thermia Oil B. Among these, the highest first and second law efficiency is noticed in parabolic dish collectors with working mediums such as water–CuO nanofluid and Thermia Oil B–CuO nanofluid, respectively. Furthermore, depending on economic analysis, it is claimed that the levelized cost of electricity for parabolic dish collectors was 28.7% less for water–Al_2O_3 nanofluid in comparison to water–CuO nanofluid. The long-term performance assessment (in terms of produced thermal energy and solar fraction) of nanofluid-based solar collectors for heating application is carried out by Harrabi et al. (2021). TRNSYS (commercial software) is used for estimating the performance assessment of the solar collector. The environmental impact is also estimated considering collected energy gain, and based on the analysis, it is claimed that the use of nanofluid (water–Al_2O_3) can reduce the emission of a greenhouse gas like CO_2 to a great extent by 0.38 t per year in Quebecois climate. Colangelo et al. (2017) have used the RadTherm (a commercial software) to estimate the influence of Al_2O_3 nanoparticle concentration on the efficiency of the solar collector. With the 3% volume fraction of nanoparticles, the thermal efficiency of the collector increased by 7.54% in comparison to the collector with bi-distilled water as a working fluid. There are different problems such as sedimentation, stability, etc., and these problems have been studied for Al_2O_3–Therminol nanofluids by Colangelo et al. (2016). The temperature while preparing the sample plays an important role in the stability of the Al_2O_3–Therminol nanofluids, and the long-term stability of nanofluids can be maintained with the presence of surfactants. Whereas, the sedimentation increases with the decrease of temperature during the mixing of Al_2O_3–Therminol nanoparticles with the help of a magnetic stirrer. The sedimentation phenomenon increases drastically with the clustering size of the nanoparticles (Iacobazzi et al. 2019). Few studies were carried out on the design modification of solar collectors by Matrawy and Farkas (1997) and Kang et al. (2017). The comparison between parallel-tube, Serpentine-tube, and two parallel plates SC for water heating application has been done by Matrawy and Farkas (1997), and it is found that the SC with parallel plate results in relatively higher efficiency which is 10% and 6% more than the parallel-tube and serpentine-tube SC, respectively. Kang et al. (2017) has also proposed and compared the flat plate SC with a U-tube collector. It is claimed that under a similar flow medium (i.e., Al_2O_3–water), the efficiency of flat-plate SC found is 14.8%, which is higher than the U-tube solar collector (with a value of 10.7%).

Visconti et al. (2016) have designed a programmable electronic system that monitors the environmental parameters (like temperature, light sensing, etc.) and also manages the electrical function to operate the external equipment to optimize the performance of the thermo-solar plant. With the use of Al_2O_3-based nanofluid, the efficiency of the solar plant increases, and in comparison to the conventional solar plant, higher performance is obtained.

In context to the literature, the suspension of nanoparticles with better thermal conductivity in base fluid results in significant improvement in thermophysical properties of the base fluid which collectively gives better collector efficiency. More importantly, there is no such article in the literature that analyzed the impact of using corrugated absorber plates in the solar water heater. This reason motivated the present investigation, and this is the novelty of the work that corrugated absorber plate is used in solar water heater instead of a flat plate. For improving the thermophysical properties of the base fluid, the nanoparticles of alumina are suspended in it. Therefore, in the present investigation, the effect of both nanofluid and corrugated absorber plate has been investigated on the heat transfer characteristics and collector efficiency. The analysis was carried out using commercial computational fluid dynamic (CFD) code with the help of the Eulerian–Eulerian (two-phase flow) model under transient conditions. This study helps for fulfilling the following objectives:

i. For understanding the heat transfer rate variation with and without the nanoparticles in the solar water heater.
ii. Among flat-plat and corrugated-plate which one is effective and gives better results.

Problem formulation

The SC considered in the present investigation consists of a corrugated-shape absorber plate, copper riser tube, and nanofluid (in which Al_2O_3 particles are suspended in the water). The constructional details of modeled SC are shown in Table 1. The flow rate within the riser tube is kept below 0.016 kg s^{-1} to ensure the homogenous distribution of temperature (Facao 2015). For effective utilization of the available computational facilities, only a single rise tube is assumed to be attached underneath of absorber plate and the schematic of the proposed SC is presented in Fig. 1.

Furthermore, the computational domain is designed using a plane of symmetry boundary condition, and thus, simulations have been performed for the half portion of

Table 1 Specification of the modeled SC

Parameter	Specification
Collector dimensions	
Length of absorber plate (L_p)	1 m
Width of absorber plate (W_p)	0.1 m
Thickness of absorber plate (T_p)	0.5×10^{-3} m
Riser tube diameter (D_r)	12.5×10^{-3} m
Riser tube thickness (t)	1×10^{-3} m
Properties of absorber plate	
Thermal conductivity	3.86×10^{2} W m − 1 K^{-1}
Density	8.9×10^{3} kg m^{-3}

the geometry. The CFD-based model was developed to estimate the thermal efficiency of the proposed SC under the following assumptions:

i. The considered nanofluid is assumed to be laminar, incompressible, spherical, and chemically non-reactive.
ii. The scattering effect for base fluid, i.e., water, is negligible.
iii. The solar radiation incident is perpendicular to the absorber plate with an intensity of 800 Wm^{-2}.
iv. The temperature rises in SC are limited to normal values, and due to this, the variation in thermophysical and optical properties is assumed to be negligible.
v. The corrugated absorber plate is assumed to be in thermal equilibrium with the working medium due to negligible thickness.
vi. The nanoparticles of Al_2O_3 are stable in water under thermal conditions and there is no slip.

Mathematical modeling

The Eulerian–Eulerian two-phase approach is used for simulating the thermal and flow characteristics in the proposed SWH. The alumina nanoparticles of size 30 nm are suspended in the water with a volume concentration (i.e., volume fraction; φ) of 1%. The flow and heat transfer equations for base fluid (i.e., water) and nanoparticles are defined separately with the help of the Eulerian–Eulerian approach and solved separately to understand the flow dynamics of the nanoparticles and base fluid, separately, so that, the behavior of nanoparticles can be understood in the base fluid. For solving the defined set of governing equations, the commercial ANSYS Fluent package has been used. The steps of the procedure for solving the problem are given in the following:

a. First of all, the conservative equations are integrated over the control volume.
b. Conversion of integral equations into the algebraic equations by using appropriate discretization techniques.
c. Find the solution by solving algebraic equations with appropriate iterative techniques and boundary conditions.

The governing equations for the present problem can be expressed as:

$$\nabla\left(\phi_i\rho_i\vec{V}_i\right)=0 \tag{1}$$

where φ_i, ρ_i, and v_i are the volume fraction, density, and velocity of the ith phase.

The volume of the ith phase can be expressed as

$$Vol_i=\int\phi_i\partial Vol \tag{2}$$

The relation between both the phases, i.e., water and nanoparticles, can be developed with the help of volume concentration which can be expressed as:

$$\phi_w+\phi_p=1 \tag{3}$$

The momentum equation for base fluid can be expressed as

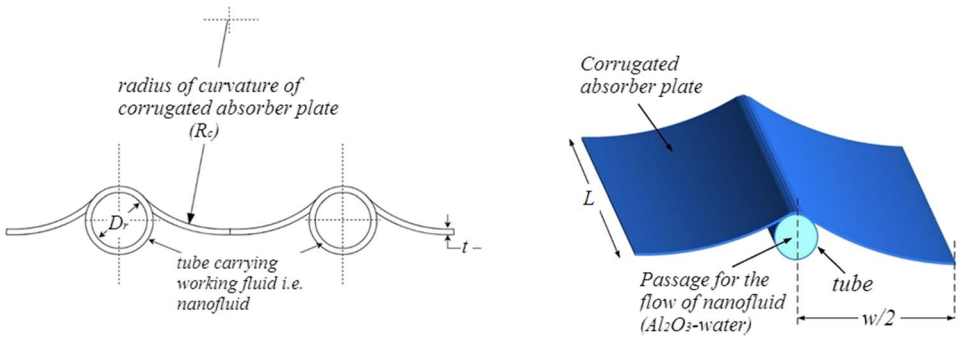

Fig. 1 Schematic of the proposed design and its computational domain for analysis

i. Proposed design of solar-assisted water heaters

ii. Computational domain of the proposed design

$$\nabla.\left(\phi_w\rho_w\vec{v}_w\vec{v}_w\right)+\left(\phi_w\nabla P\right)=\nabla.\left(\phi_w\mu_w\nabla\vec{v}_w\right)+K_{wn}\left(\vec{v}_p-\vec{v}_w\right) \tag{4}$$

Similarly, for nanoparticles, the momentum equation can be written as:

$$\nabla.\left(\phi_n\rho_n\vec{v}_n\vec{v}_n\right)+\left(\phi_n\nabla P\right)=\nabla.\left(\phi_n\mu_n\nabla\vec{v}_n\right)+K_{wn}\left(\vec{v}_p-\vec{v}_w\right) \tag{5}$$

where K_{wn} is the coefficient of momentum exchanger between both the phases, and it can be calculated as:

$$K_{wn}=\frac{3}{4}\left(\phi_w\phi_n\rho_nC_D\mathrm{Re}_n\right)\times\frac{\mu_w}{\rho_nd_n^2} \tag{6}$$

In Eq. (6), the C_D is estimated based on the Schiller and Naumann model (1935) and Re_n can be calculated using following relation:

$$\mathrm{Re}_n=\frac{\rho_w}{\mu_w}d_n\left|\vec{v}_n-\vec{v}_w\right| \tag{7}$$

The thermal behavior of the base and nanoparticles is modeled by defining separate equation for both the phases, and these equations are:

$$\nabla.\left(\phi_w\rho_wh_w\vec{v}_w\right)=\left(\phi_w\mu_w\nabla\vec{v}_w\right):\nabla\vec{v}_w-\nabla.\vec{q}_w+h_v\left(T_w-T_n(\text{for base}-\text{fluid})\right) \tag{8}$$

$$\nabla.\left(\phi_n\rho_nh_n\vec{v}_n\right)=\left(\phi_n\mu_n\nabla\vec{v}_n\right):\nabla\vec{v}_n-\nabla.\vec{q}_n+h_v\left(T_w-T_n\right)(\text{for nanoparticles}) \tag{9}$$

In Eqs. (8) and (9), the h_v is the coefficient of volumetric heat transfer and it can be calculated as:

$$h_v=\left(6Ck_w\phi_w\phi_n\right)\times\frac{Nu_n}{d_n^2} \tag{10}$$

where C is the constant and it can be calculated based on Re and volume fraction (φ). The expression for estimation of C is:

$$C=10^{-9}\times\left(\left|5.505-9.606\times10^{-6}\mathrm{Re}^2+1.539\times10^{-2}\mathrm{Re}-3.973\times10^2\phi\right|\right) \tag{11}$$

The heat transfer associated with the nanoparticles can be estimated using the correlation developed by Ranz and Marshall (1952).

Thermophysical properties of nanofluid

With the suspension of nanoparticles in the base fluid, the thermophysical properties of the fluid improved considerably which leads to the better overall performance of the SC.

The density of the nanofluid is predicted using the following expression:

$$\rho_n=\rho_w(1-\phi)+\left(\rho_n\times\phi\right) \tag{12}$$

where ρ_w and ρ_n presents the density of the base fluid (i.e., water) and nanoparticles, respectively. φ is calculated using the expression (Azmi et al. 2013):

$$\varphi=\left[\frac{\left(\omega\times\rho_w\right)}{(1-0.01\times\omega)+(0.01\times\omega)\rho_w}\right] \tag{13}$$

The correlation developed by Pak and Cho (1998) has been used for calculating the viscosity of the nanofluid:

$$\frac{\mu_n}{\mu_w}=\left[1+39.11\phi+533.9\phi^2\right] \tag{14}$$

For estimating the thermal conductivity of the nanofluid, the correlation developed by Khanafer and Vafai (2011) is used, and it can be written as:

$$k_n=k_f\left[1+1.0112\phi+2.4375\phi\times\left(\frac{47}{d_n}\right)-0.0248\phi\times\left(\frac{K_B}{0.613}\right)\right] \tag{15}$$

where K_B is the Stefan–Boltzmann constant.

Numerical simulation

The flow-governing equations for a multiphase problem have been numerically solved with the help of commercial CFD code (i.e., Fluent). The entire set of governing equations was solved via discretizing the fluid domain using the finite volume method which facilitates the conversion of partial differential equations (PDEs) into simplified algebraic equations. The Eulerian model is used for numerical modeling of the two-phase model in which the different phases are treated mathematically as interpenetrating continua and a set of governing equations were solved separately for each phase [ANSYS, Theory Guide].

In numerical simulation, convergence is one of the main concerns and for attaining the convergence, the appropriate numerical strategy is required. The flow-governing equations were solved under specified boundary conditions with the help of a pressure-based solver along with the segregated iterative scheme. The least-squares cell-based gradient scheme was considered for spatial discretization. The simulations are performed under transient conditions. The continuity and momentum equation is discretized using the upwind scheme of the second order, while the energy equation is discretized using the first-order upwind scheme. The volume fraction is discretized using a QUICK scheme. For ensuring the smooth convergence of the solution, the under relaxation factors were kept to be with default values. The convergence of the solution is determined based on the different calculated variables which

are mass, velocity, volume fraction, energy, etc., and the residual values for all the variables were considered to be 10^{-5}. In addition to this, the convergence was also determined from the mass flux report where it was checked that the net mass balance, i.e., the difference between inlet and outlet mass, must be close to zero.

Meshing and grid-independence test

The proposed SC consists of a circular pipe with a nanofluid flowing through it and the top surface of the pipe is exposed to solar radiation which causes the transfer of heat from the solar radiation to the nanofluid flowing through the pipe. There exist both solid and fluid bodies and for ensuring the accuracy in the results, the inflation of fine elements which increases at the rate of 2.5 is placed at the interface of the solid and fluid body. Thus, at the periphery of the pipe, the hexahedral meshing is created because it provides an accurate solution with less number of cells in comparison to tetrahedral mesh. It is also taken care of during the meshing that the y^+ value remains less than 1, such that the transfer of heat can be accurately modeled from the solid to the fluid body. While at the center of the pipe, the temperature gradient is marginal which allowed the creation of relatively coarse meshing with triangular-shaped elements. The schematic of meshed domain with different boundary conditions is shown in Fig. 2, and the details of element size are given in Table 2.

It is also ensured that the simulated solution is free from the number of grid elements that were generated during the meshing and that grid independence is checked at Reynolds number (*Re*) of 700 for $\phi = 5\%$. A total of six different sets of grid system with elements of 534,346, 854,295, 1,024,682, 1,396,748, 1,643,296, and 1,803,046 is examined for grid independence. Figure 3 presents the variation of nanofluid outlet temperature (T_{out}) for different grid systems. It is found that with the refinement of the grid systems, the solution progresses towards grid independence. As it can be seen that after the 1,643,296 number of elements, there is a marginal increment in the T_{out} value which is even lower than 1%. Thus, it is concluded that after 1,643,296 elements, the solution remains unaltered even further refining the grid size.

Data reduction

With the help of numerical simulations, the temperature of outlet fluid and absorber plate is estimated, and based on that, the useful energy (Q_u) is calculated under steady-state conditions. The Q_u is equaled to the difference of heat

Table 2 Details of the meshing

Body	Type of meshing	y^+ value	Number of inflation layers	Distance of first inflation layer from the adjacent body ($\times 10^{-4}$)
Fluid	Hexahedral and tetrahedral	0.95	25	0.6

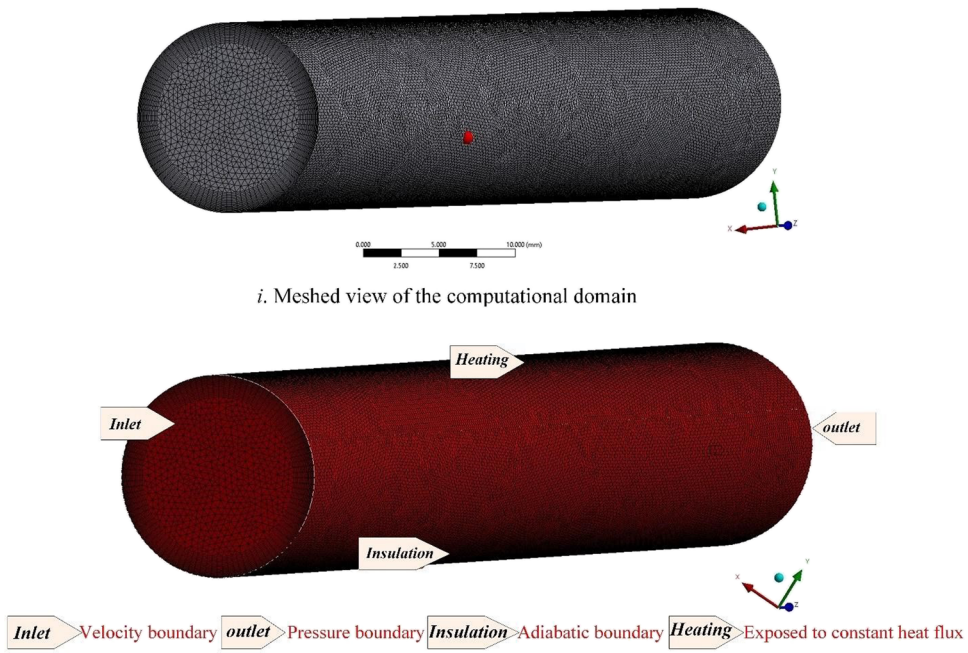

Fig. 2 Schematic presentation of different boundary conditions

i. Meshed view of the computational domain

ii. Presentation of different boundary conditions for simulating the problem

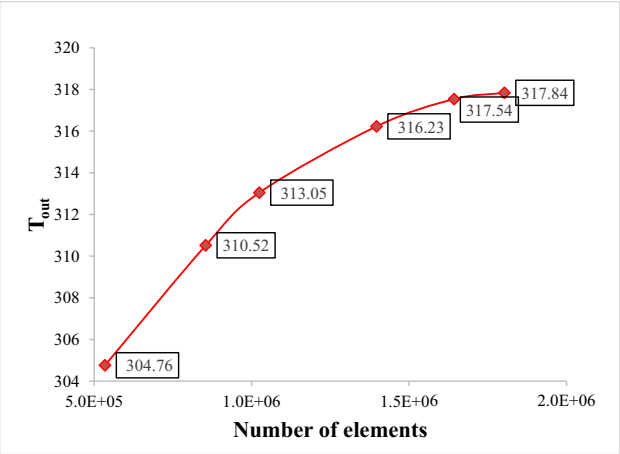

Fig. 3 Grid-independence test for outlet temperature (T_o)

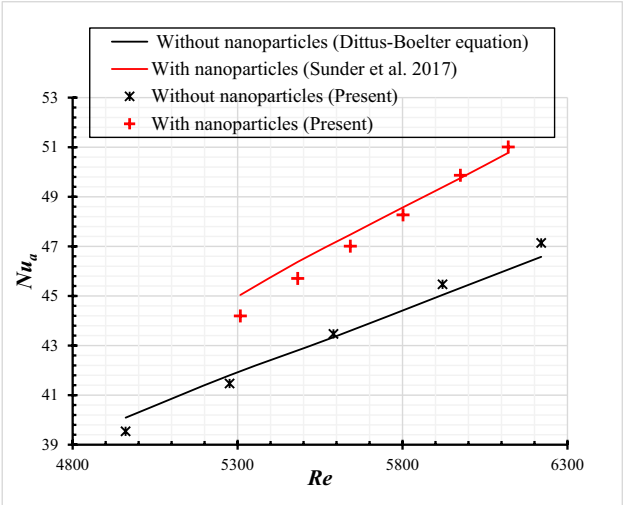

Fig. 4 Validation of model with Nasrin and Alim (2014)

received from the solar radiations (Q_r) and heat loss (Q_l) to the surrounding, i.e., atmosphere. It can be expressed as

$$Q_u = Q_r - Q_l \tag{16}$$

where

$$Q_r = IA \tag{17}$$

and

$$Q_l = hA\left(T_c - T_s\right) \tag{18}$$

where T_c and T_s are the temperatures of the collector and surrounding, respectively.

The Q_u can also be estimated from the heat that is carried away by the fluid flowing through SC, i.e.,

$$Q_u = mC_p\left(T_o - T_i\right) \tag{19}$$

The efficiency of the SC can be estimated as

$$\eta = \frac{Q_u}{Q_r} = \frac{mC_p\left(T_o - T_i\right)}{AI} \tag{20}$$

The average Nusselt number (Nu_a) depends on heat capacity, thermal conductivity, viscosity, volume fraction, etc., and it can be calculated as:

$$Nu_a = -\frac{k_n}{k_f} \times \frac{\partial \theta}{\partial y} \tag{21}$$

where

$$\theta = \frac{\left(T_o - T_i\right)}{k_f \times Q} \tag{22}$$

Validation

The validation is the most important part of the numerical simulation in which the predicted results are compared with the well-established finds. In the present study, the input parameter, i.e., heat flux of solar radiation (I_s), inlet fluid temperature (T_i), mass flow rate of fluid at the inlet (m), and atmospheric temperature (T_a) was used, and based on these parameters, the output parameters, i.e., absorber plate (T_p) and outlet fluid temperature (T_o), are predicted under steady state. The validation of the numerical model has been carried out in two different steps: preliminary with the Dittus–Boelter equation (provided in Eq. 13) while it is considered that water is the working fluid in SC; final results of the nanofluid-based SC were validated with the experimental findings of the Sundar et al. (2017).

Equation (13) is applicable to validate the results when the working fluid is only water, and the results of the comparison are summarized in Fig. 4. It is noticed that the adopted numerical methodology predicts results that match closely with the Nu_a calculated using Eq. (13) with a maximum deviation of less than ± 5%. In the second step, the proposed methodology for nanofluid is validated with the experimental findings of Sundar et al. (2017), and during this, the water properties were replaced with the Al_2O_3 nanofluid having a volume fraction of 0.1%. With the use of Al_2O_3 nanofluid, the Nu_a improved by 6.26% at Re of 5000 in comparison to water SC. At a similar volume fraction, the numerically simulated results of Nu_a have been compared with the results of Sundar et al. (2017) and the results are presented in Fig. 4. Compared results have shown a good match between each other with a maximum

error of less than ± 6.5%, and thus, the proposed numerical methodology was found to be suitable for further analysis.

Results and discussion

The CFD model of the proposed SC is designed to understand the effect of the radius of curvature (RC) of the corrugated absorber plate on the outlet temperature (T_o) of the water–Al_2O_3 nanofluid, Nusselt number (Nu_a), and collector efficiency (η). The numerical data is collected under steady-state conditions for *Re* ranging from 300 to 1500.

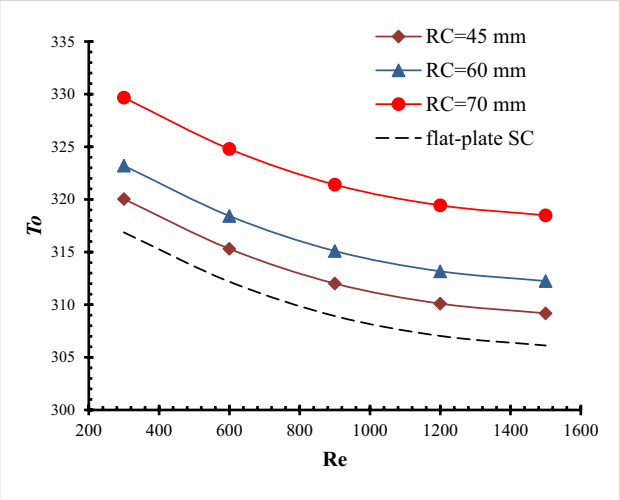

Fig. 5 Variation of T_o with RC

The volume fraction (ϕ) of nanoparticles in the water is kept constant, i.e., 1%.

Figure 5 presents the variation of T_o with Re for various RC values. It is noticed that with an increase in flow rate, the T_o decreases considerably. Furthermore, there is a remarkable change in T_o found with the variation of RC from 45 to 70 mm in three configurations. The minimum T_o is obtained in the case of conventional flat-plate SC, and it decreases with the decrease of RC from 70 to 45 mm. The nanoparticles which were presented in the fluid rapidly get heated up (due to relatively low velocity in the base fluid and with higher thermal conductivity in comparison to the base fluid) and attain the temperature as that of the absorber plate (Nasrin and Alim 2014). Because of this, the T_o obtained in the nanofluid is comparatively higher than the normal SC. As the overall thermal conductivity of working fluid increased with the suspension of nanoparticles, it allows more thermal energy from the corrugated absorber plate in comparison to the simple flat-plate SC. This creates a higher temperature region near the interface of absorber plate and nanofluid as it can be seen in Fig. 6. Furthermore, for an effective SC design, the T_o should need to be as close as possible to the absorber plate temperature because this indicates that the maximum heat is extracted from the absorber plate to the nanofluid which flows through the riser tube (Gunjo et al. 2017). Besides this, it keeps the absorber plate temperature low which resulted in low heat loss from the glass cover to the surrounding (Kasaeian et al. 2015). In the case of flat-plate SC, the absorber plate is flat and there is a line of contact that takes place between

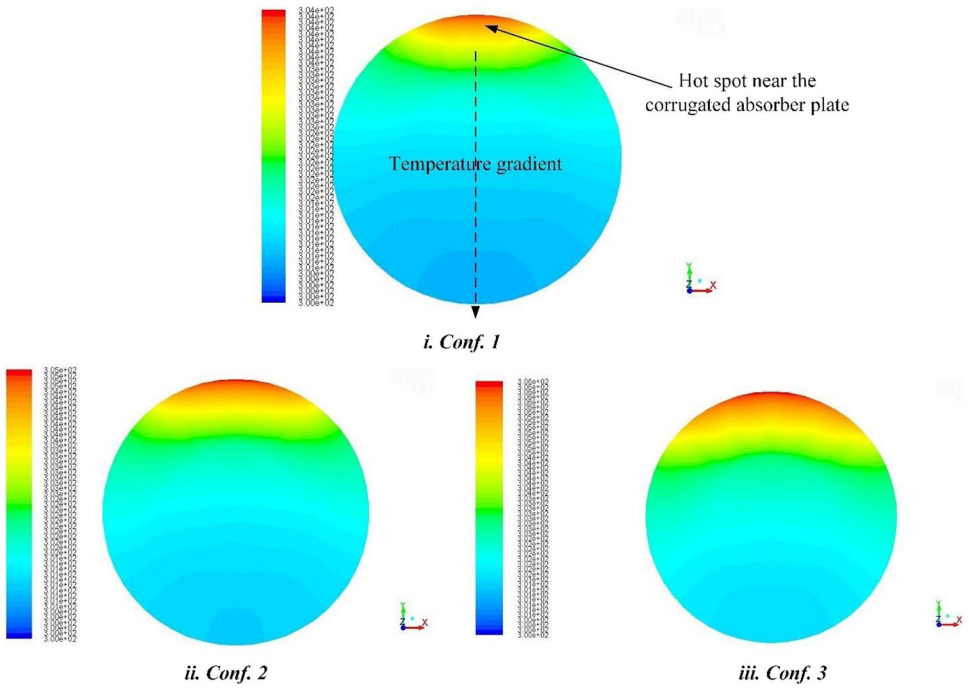

Fig. 6 Variation of the temperature profile in different configurations

the absorber plate and the riser tube. But, with the proposed SC, the contact area between the absorber plate and the rise tube is increased, which helps the rise tube to extract more amount of heat from the absorber plate, and thus, the T_o increases.

The effect of using a corrugated absorber plate on heat transfer is studied based on Nu_a. Figure 7 depicts the plot of Nu_a vs Re for different RC values. At lower Re, the Nu_a is comparatively low and it is increasing significantly with the increase of Re from 300 to 1500. The augmentation in heat transfer occurred due to the fact that with the increase of Re, the sedimentation of the nanoparticles in the base fluid decreased, and therefore, the nanoparticles take effective part in the heat extracted from the absorber plate of the SC. In comparison to water-based SC, there is a remarkable augmentation in Nu_a noticed in the proposed SC with water–Al_2O_3 as a working fluid. Moreover, the RC variation also shown a good improvement in Nu_a. The corrugated absorber plate also improves the heat transfer area between the absorber plate and tube. Due to this, there is a better heat transfer from the tube to the working fluid, and thus, an increase in Nu_a is noticed. This fluctuation in Nu_a occurred due to the presence of nanoparticles of aluminum oxide in the water solution. With the suspension of these nanoparticles, the thermophysical properties (especially thermal conductivity) get improved which allow nanofluid to capture, gather, and transfer thermal energy easily with the surrounding fluid molecules. Due to this, the heat convection rate improves remarkably in the riser tube (Takabi and Shokouhmand 2015). The thermal conductivity of the working flow improved considerably, and it leads to a better augmentation of Nu_a in the SC. The maximum augmentation in Nu_a has occurred in the case of RC = 70 mm, which is approximately 69% higher than the pure water-based SC.

The effectiveness of the SC can only be measured based on efficiency which is defined as the ratio between useful heat gain (Q_u) and available solar energy (Q_r). The useful heat gain using the SC can be easily calculated from the amount of heat that was carried out by the working fluid which flows through the SC. Figure 8 shows the variation of SC efficiency (η_c) with Re. The η_c increases considerably with the variation of Re from 300 to 1500. In comparison to flat-plate SC, the η_c found in corrugated plate SC is approximately 14% higher under a similar nanofluid. This happens due to the increase in Q_u due to increasing the available heat transfer area by providing a corrugated absorber plate. With the variation of RC from 45 to 70 mm, the contact area between the tube and absorber plate increases, and due to this reason, the available heat transfer for the tube is increased. Moreover, the nanoparticles present in the water (i.e., base-fluid) improve the thermal conductivity of the working medium, i.e., nanofluid which increases the rate of heat transfer from the corrugated absorber plate to the adjacent nanofluid flowing through the riser tube. Therefore, considerable augmentation in Q_u takes place. Because of this reason, the thermal efficiency (η_c) of the SC increases.

The Nu_a calculated for the proposed SC is compared with the results presented by Sandhu (2013), and the results of the comparison are shown in Fig. 9. In comparison to the results presented by Sandhu (2013), the Nu_a found in the proposed SC is approximately 43% higher at Re of 1400. Due to this, it is concluded that the corrugated plate SC is a better option than the flat-plate SC. The presented design of SC gives higher Nu_a along with η_c in comparison to flat-plate SC, and the reason for the same is the higher available heat transfer area in the proposed SC.

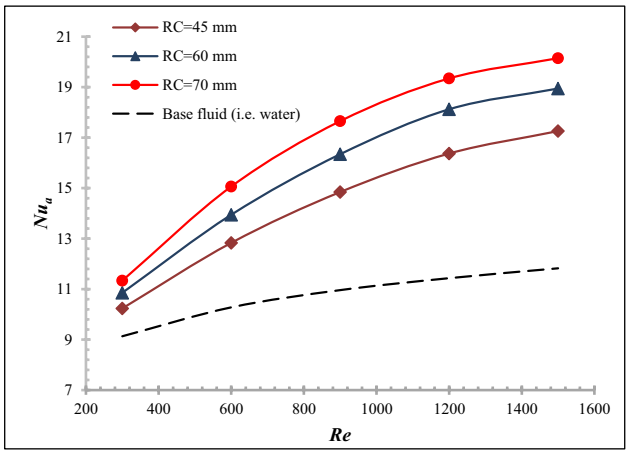

Fig. 7 Nu_a vs Re for different RC values

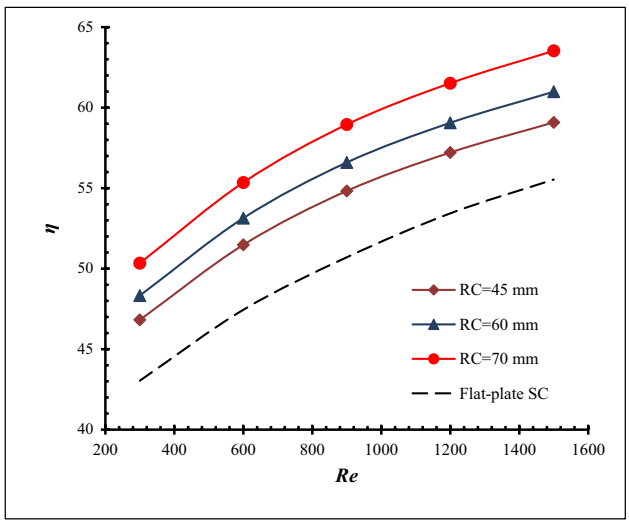

Fig. 8 Variation of η with RC

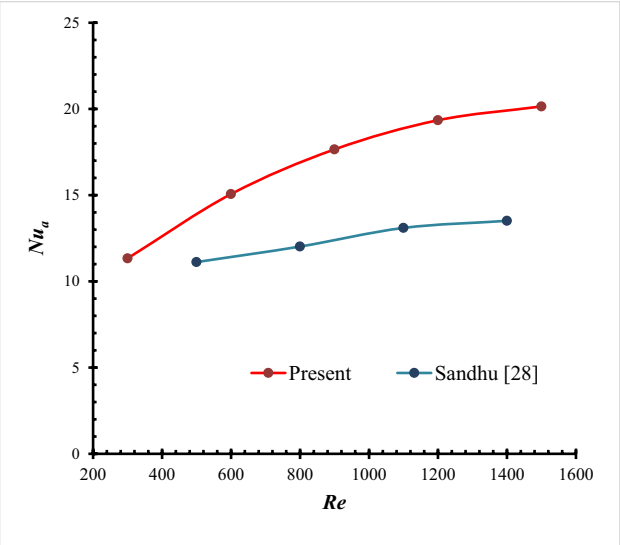

Fig. 9 Comparison of Nu_a with Sandhu (2013)

Conclusion

The influence of radius of curvature (*RC*) of corrugated plate solar collector is studied with the help of commercial ANSYS (Fluent) software. The base working fluid is suspended with the Al_2O_3 nanoparticles to improve the thermophysical properties of the SC. The numerical simulations lead to the following conclusions:

1. By using the corrugated plate instead of the flat plate, the available heat transfer area for the useful heat gain increases remarkably which gives better performance.
2. The corrugated plate increases the augmentation of heat through the solar collector in comparison to the flat plate.
3. In comparison to the flat-plate solar collector, the heat transfer found in the proposed SC is approximately 43% higher at *Re* of 1400.
4. The collector efficiency found in corrugated plate SC is approximately 14% higher than the flat-plate one.

Author contribution Rajneesh Kumar: methodology and simulations, investigation, writing—original draft, language, and review-editing. Manjeet Khurab: assisted in writing and data extraction, and referencing. Rajesh Sharma: arranged computational facility, language and review-editing. Periapattana Nagaraj Hrisheekesha: language editing and proofreading. Varun Goel: result validation, proofreading, and review-editing. Suvanjan Bhattacharyya: proofreading and review-editing. Vineet Veer Tyagi: proofreading and review-editing. Varun: assisted in writing and data extraction, and referencing.

Data availability NA

Declarations

Ethical approval Hereby, I (Dr. Rajneesh Kumar) consciously assure that for the manuscript *A novel design for solar collector used for water heating application having nanofluids as working medium: CFD modeling and simulation,* the finding presented in this research report is the authors' work, which has not been previously published elsewhere and the manuscript in part or in full has not been submitted or published anywhere.

Consent to participate All the authors contributed their paper in writing this manuscript.

Consent to publish With the mutual agreement of all the authors, it is decided that if this manuscript is accepted by the Editor-in-Chief, it will be published in the Environmental Science and Pollution Research Journal.

Conflict of interest The authors declare no competing interests.

References

Abo-Elfadl S, El-Dosoky MF, Hassan H (2021) Energy and exergy assessment of new designed solar air heater of V-shaped transverse finned absorber at single- and double-pass flow conditions. Environ Sci Pollut Res 28: 69074–69092. https://link.springer.com/article/10.1007/s11356-021-15163-z

Ali A, Vafai K, Khaled ARA (2003) Comparative study between parallel and counter flow configuration between air and falling film desiccant in the presence of nanoparticles suspensions. Int J Energy Res 27:725–745

Azari P, Lavasani AM, Rahbar N, Yazdi ME (2021) Performance enhancement of a solar still using a V-groove solar air collector—experimental study with energy, exergy, enviroeconomic, and exergoeconomic analysis. Environmental Science and Pollution Research 28: 65525–65548. https://link.springer.com/article/10.1007/s11356-021-15290-7

Azmi WH, Sharma KV, Sarma PK, Mamat R, Anuar S, Rao VD (2013) Experimental determination of turbulent forced convection heat transfer and friction factor with SiO2 nanofluid. Exp Thermal Fluid Sci 51:103–111. https://doi.org/10.1016/j.expthermflusci.2013.07.006

Choi US (1995) Enhancing thermal conductivity of fluid with nanoparticles. ASME FED 231: 99–103. https://www.osti.gov/biblio/196525

Colangelo G, Favale E, Miglietta P, Milanese M, De Risi A (2016) Thermal conductivity, viscosity and stability of Al_2O_3-diathermic oilnanofluids for solar energy systems. Energy 95:124–136. https://doi.org/10.1016/j.energy.2015.11.032

Colangelo G, Milanese M, De Risi A (2017) Numerical simulation of thermal efficiency of an innovative al2o3 nanofluid solar thermal collector:influence of nanoparticles concentration. Therm Sci 21(6):2769–2779. https://doi.org/10.2298/TSCI151207168C

Das SK, Choi US, Patel HE (2006) Heat transfer in nanofluids - a review. Heat Transfer Eng 27:3–19. https://doi.org/10.1080/01457630600904593

Eastman JA, Choi SUS, Li S, Yu W, Thompson IJ (2001) Anomalously increased effective thermal conductivities of ethylene glycol-based nanofluids containing copper nanoparticles. Appl Phys Lett 78:718–720. https://doi.org/10.1063/1.1341218

Eidan AA, AlSahlani A, Ahmed AQ, Al-fahham M, Jalil JM (2018) Improving the performance of heat pipe-evacuated tube solar collector experimentally by using Al2O3 and CuO/acetone nanofluids. Sol Energy 173:780–788

Facao J (2015) Optimization of flow distribution in flat plate solar thermal collectors with riser and header arrangements. Sol Energy 120:104–112. https://doi.org/10.1016/j.solener.2015.07.034

GaneshKumar P, Sakthivadivel D, Prabakaran R, Vigneswaran S, SakthiPriya M, Thakur AK, Sathyamurthy R, Kim SC (2022) Exploring the thermo-physical characteristic of novel multi-wall carbon nanotube—Therminol-55-based nanofluids for solar-thermal applications. Environ Sci Pollut Res 29:10717–10728. https://doi.org/10.1007/s11356-021-16393-x

Goel AK, Singh SN (2021) Experimental performance evaluation of an impinging jet with fins type solar air heater. Environ Sci Pollut Res 28:19944–19957

Goel V, Hans VS, Singh S, Kumar R, Pathak SK, Singla M, Bhattacharyya S, Almatrafi E, Gill RS, Saini RPb (2021) A comprehensive study on the progressive development and applications of solar air heaters. Sol Energy 229:112–147

Gunjo DG, Mahanta P, Robi PS (2017) CFD and experimental investigation of flat plate solar water heating system under steady state condition. Renewable Energy 106:24–36

Harrabi I, Hamdi M, Hazami M (2021) Long-term performances and technoeconomic and environmental assessment of Al_2O_3/water and MWCNT/Oil nanofluids in three solar collector technologies. J Nanomater: 6461895. https://doi.org/10.1155/2021/6461895

He Q, Zeng S, Wang S (2015) Experimental investigation on the efficiency of flat-plate solar collectors with nanofluids. Appl Therm Eng 88:165–171. https://doi.org/10.1016/j.applthermaleng.2014.09.053

Huang W, Marefati M (2020) Energy, exergy, environmental and economic comparison of various solar thermal systems using water and Thermia Oil B base fluids, and CuO and Al2O3 nanofluids. Energy Rep 6:2919–2947. https://doi.org/10.1016/j.egyr.2020.10.021

Iacobazzi F, Milanese M, Colangelo G, Lomascolo M, Risi A (2016) An explanation of the Al2O3 nanofluid thermal conductivity based on the phonon theory of liquid. Energy 116:786–794. https://doi.org/10.1016/j.energy.2016.10.027

Iacobazzi F, Milanese M, Colangelo G, De Risi A (2019) A critical analysis of clustering phenomenon in Al2O3 nanofluids. J Therm Anal Calorim 135:371–377. https://doi.org/10.1007/s10973-018-7099-9

International Renewable Energy Agency (IRENA) (2018) Data and statistics – IRENA resource. http://resourceirena.irena.org/gateway/dashboard/?topic¼4&subTopic¼417. Accessed 20 Dec 2021

Jobair HK, Abdullah OI, Atyia Z (2018) Feasibility study of a solar flat plate collector for domestic and commercial applications under Iraq climate. J Phys Conf 012005. https://iopscience.iop.org/article/10.1088/1742-6596/1032/1/012005/meta

Kalogirou S (2009) Solar energy engineering: processes and systems. Academic Press

Kang W, Shin Y, Cho H (2017) Economic analysis of flat-plate and U-tube solar collectors using an Al2O3 nanofluid. Energies 10:1911. https://doi.org/10.3390/en10111911

Kasaeian A, Eshghi AT, Sameti M (2015) A review on the applications of nanofluids in solar energy systems. Renew Sustain Energy Rev 43:584–598

Khanafer K, Vafai K (2011) A critical synthesis of thermophysical characteristics of nanofluids. Int J Heat Mass Transf 54:4410–4428. https://doi.org/10.1016/j.ijheatmasstransfer.2011.04.048

Kumar R, Goel V, Kumar A (2020) A note on the comparative analysis between rectangular and modified duct heat exchanger. J Heat Transfer 142:041901. https://doi.org/10.1115/1.4045755

Matrawy KK, Farkas I (1997) Comparison study for three types of solar collectors for water heating. Energy Convers Manage 38:861–869. https://doi.org/10.1016/S0196-8904(96)00089-1

Michael JJ, Iniyan S (2015) Performance of copper oxide/water nanofluid in a flat plate solar water heater under natural and forced circulations. Energy Convers Manage 95:160–169. https://doi.org/10.1016/j.enconman.2015.02.017

Milanese M, Iacobazzi F, Colangelo G, Risi A (2016) An investigation of layering phenomenon at the liquid–solid interface in Cu and CuO based nanofluids. Int J Heat Mass Transf 103:564–571. https://doi.org/10.1016/j.ijheatmasstransfer.2016.07.082

Nasrin R, Alim MA (2014) Semi-empirical relation for forced convective analysis through a solar collector. Sol Energy 105:455–467. https://doi.org/10.1016/j.solener.2014.03.035

Natarajan E, Sathish R (2009) Role of nanofluids in solar water heater. Int J Adv Manuf Technol. https://doi.org/10.1007/s00170-008-1876-8

Pak BC, Cho Y (1998) Hydrodynamic and heat transfer study of dispersed fluids with submicron metallic oxide particles. Experimental Heat Transfer 11:151–170

Pang C, Jung JY, Lee JW, Kang YT (2012) Thermal conductivity measurement of methanol-based nanofluids with Al2O3 and SiO2 nanoparticles. Int J Heat Mass Transf 55:5597–5602

Ranz W, Marshall W (1952) Evaporation from drops. Chem Eng Prog 48:141–146

Sasikumar SB, Santhanam H, Noor MM, Devasenan M, Ali HM (2020) Experimental investigation of parallel type -evacuated tube solar collector using nanofluids. Energy Sources (Part A): https://doi.org/10.1080/15567036.2020.1829201

Schiller L, Naumann Z (1935) A drag coefficient correlation. Z Ver Deutsch Ing 77:318–323

Shafahi M, Bianco V, Vafai K, Manca O (2010) An investigation of the thermal performance of cylindrical heat pipes using nanofluids. Int J Heat Mass Transf 53:376–383. https://doi.org/10.1016/j.ijheatmasstransfer.2009.09.019

Sandhu G (2013) Experimental study of temperature field in flat-plate collector and heat transfer enhancement with the use of insert devices. M. of Engg. Sci. theseis, The School of Graduate and Postdoctoral Studies, The University of Western Ontario London, Ontario

Sundar LS, Bhramara P, Kumar NTR, Singh MK, Sousa ACM (2017) Experimental heat transfer, friction factor and effectiveness analysis of Fe_3O_4 nanofluid flow in a horizontal plain tube with return bend and wire coil inserts. Int J Heat Mass Transf 109:440–453

Sundar LS, Sintie YT, Said Z, Singh MK, Punnaiah V, Sousa A, Sousa ACM (2020) Energy, efficiency, economic impact, and heat transfer aspects of solar flat plate collector with Al2O3 nanofluids and wire coil with core rod inserts. Sustain Energy Technol Assess 40:100772. https://doi.org/10.1016/j.seta.2020.100772

Takabi B, Shokouhmand H (2015) Effect of Al_2O_3-Cu/water hybrid nanofluid on heat transfer and flow characteristics in turbulent regimes. Int J Mod Phys C 26:1550047

Visconti P, Primiceri P, Costantini P, ColangeloyG G, Cavalera, (2016) Measurement and control system for thermosolar plant and performance comparison between traditional and nanofluid solar thermal collectors. Int J Smart Sens Intell Syst 9:1220–1242

World Energy Outlook 2019, 2019

Xuan Y, Li Q (2020) Heat transfer enhancement of nanofluids. Int J Heat Fluid Flow 21:58–64. https://doi.org/10.1016/S0142-727X(99)00067-3

Zhu DS, Wu SY, Yang S (2011) Numerical simulation on thermal energy storage behavior of SiC-H2O nanofluids. Energy Sources (Part A) 33:1317–1325